ELSEVIER

www.elsevier.nl/locate/jorganchem

Journal of Organometallic Chemistry 583 (1999) 56–62

Journal of Organometallic Chemistry

Kinetic study of the alkylation of cyanide at $[NBu_4][trans\text{-}Re(CN)_2(dppe)_2]$. Crystal structures of $[NBu_4][trans\text{-}Re(CN)_2(dppe)_2]$ and $trans\text{-}[Re(CN)_2(dppe)_2]$☆

M. Fernanda N.N. Carvalho [a], M. Teresa Duarte [a], Adelino M. Galvão [a], Armando J.L. Pombeiro [a,*], Richard Henderson [b], Hartmut Fuess [c], Ingrid Svoboda [c]

[a] *Centro de Química Estrutural, Complexo I, Instituto Superior Técnico, Av. Rovisco Pais, 1049-001 Lisbon, Portugal*
[b] *Nitrogen Fixation Laboratory, John-Innes Centre, Norwich Research Park, Colney Lane, Norwich NR4 7UH, UK*
[c] *Strukturforschung, FB Materialwissenschaft, Technische Universität, Petersenstrasse 23, 64287 Darmstadt, Germany*

Received 10 July 1998; received in revised form 28 September 1998

Abstract

The mechanism of alkylation of $[NBu_4][trans\text{-}Re(CN)_2(dppe)_2]$ (**1**) by alkyl iodides (RI; R = Me, Et or Pr) or EtBr was studied by stopped-flow techniques, which indicate that it involves a fast first alkylation to give $trans\text{-}[Re(CN)(CNR)(dppe)_2]$ that undergoes a subsequent relatively slow alkylation at the cyano-ligand with a rate constant that decreases with the increase of the carbon chain length of the R group and with the replacement of iodide by bromide in the organohalide. Sodium iodide inhibits the rates of alkylation, probably by forming ion pairs with $trans\text{-}[Re(CN)_2(dppe)_2]^-$ as confirmed by the formation of the adducts $[Re(CN)(CNM)(dppe)_2]$ (M = Li, Na, Tl or Ag) by reaction of **1** with convenient metal salts and by the kinetics of the reaction between MeI and $[Re(CN)(CNNa)(dppe)_2]$. The X-ray molecular structures of $[NBu_4][trans\text{-}Re(CN)_2(dppe)_2]$ and $trans\text{-}[Re(CN)_2(dppe)_2]$ confirm they have pseudo octahedral geometries and indicate that the former crystallizes in the triclinic $P\bar{1}$ space group with $a = 17.938(2)$, $b = 18.473(3)$, $c = 20.061(3)$ Å and the latter in the monoclinic space group $P2_1/c$ with $a = 11.673(2)$, $b = 13.302(3)$, $c = 17.166(4)$ Å.

Keywords: Alkylation; Kinetic studies; Stopped flow spectrophotometry; Cyanide; Isocyanide; Organohalide; Rhenium; X-ray analyses

1. Introduction

It was previously demonstrated [1] that cyanide coordinated at $[NBu_4][trans\text{-}Re(CN)_2(dppe)_2]$ (**1**) is readily alkylated, by species such as $[Et_3O][BF_4]$ or RI (R = Me, Et or Pr), affording the bis-isocyanide species $trans\text{-}[Re(CNR)_2(dppe)_2]^+$. However, it remained unknown if the process involved electrophilic attack at the electron-rich anionic centre or direct attack on the cyanide ligand, as well as the effect of the R moiety or the halide character on the kinetics. We now report a kinetic study of this process and of that of the $[Re(CN)(CNNa)(dppe)_2]$ adduct.

The crystal structures of the first complex and of that readily derived upon oxidation, $trans\text{-}[Re(CN)_2(dppe)_2]$, are also reported.

2. Results and discussion

2.1. Kinetic studies for the alkylation of the dicyano-complex

The reactions of $[NBu_4][trans\text{-}Re(CN)_2(dppe)_2]$ (**1**) with alkyl halides (RX; X = I, R = Me, Et or Pr. X = Br, R = Et) (Eq. (1)) were studied by stopped-flow spectrophotometry at $\lambda = 400$ nm in THF, using at least a tenfold excess of the alkylating agent.

☆ Dedicated to Professor Alberto Ceccon on the occasion of his 65th birthday.

* Corresponding author. Tel. + 351-1-841-9237; fax: + 351-1-846-4455/4457.

E-mail address: pombeiro@alfa.ist.utl.pt (A.J.L. Pombeiro)

0022-328X/99/$ - see front matter
PII: S0022-328X(99)00113-8

$$[NBu_4][\underset{(1)}{trans\text{-}Re(CN)_2(dppe)}]_2 + 2RX \rightarrow trans\text{-}[Re(CNR)_2(dppe)_2]X + [NBu_4]X \quad (1)$$

The absorbance versus time traces have an initial absorbance (A_i) slightly lower than that of the precursor cyanide complex (A_0) and close to that of the mixed cyanide–isocyanide intermediate *trans*-$[Re(CN)(CNR)(dppe)_2]$ ($A_i = 0.42$, for R = Me, see Fig. 1). The final absorbance $A_\infty = 0.13$, R = Me) is in good agreement with that of the dialkylated complex *trans*-$[Re(CNR)_2(dppe)_2]^+$. The traces are an excellent fit to a single exponential curve as shown in Fig. 1.

The exponential nature of the curves is consistent with a first order dependence on the concentration of the complex (**1**). This was confirmed by observing that k_{obs} was unaffected by varying the complex concentration (in the 1×10^{-4}–5×10^{-3} mol dm^{-3} range), at a constant concentration (1×10^{-3} mol dm^{-3} or 50×10^{-3} mol dm^{-3}) of the alkylating agent. The dependence on the concentration of RX is first order as shown in Fig. 2, for the reaction with MeI.

The observed behaviour is in agreement with a fast first alkylation process occurring within the dead-time (2 ms) of the apparatus (reaction 2), followed by the second alkylation process (reaction 3) which is the reaction being monitored.

$$[NBu_4][\underset{(1)}{trans\text{-}Re(CN)_2(dppe)}]_2 + RX \xrightarrow{k_1} [Re(CN)(CNR)(dppe)_2] + [NBu_4]X \quad (2)$$

$$[Re(CN)(CNR)(dppe)]_2 + RX \xrightarrow{k_2} [Re(CNR)_2(dppe)_2]X \quad (3)$$

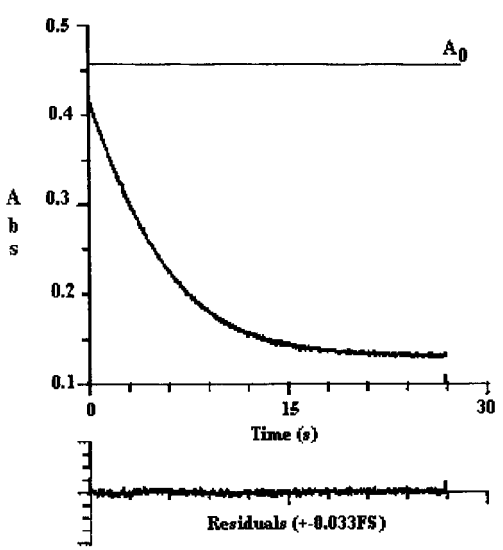

Fig. 1. Absorbance versus time dependence for the reaction of $[NBu_4][trans\text{-}Re(CN)_2(dppe)_2]$ (**1**) (1.0×10^{-4} M) with MeI (1.0×10^{-1} M), in THF at $\lambda = 400$ nm, temperature = 25°C; A_0, absorbance of complex (**1**). Curve was fitted using $k_{obs} = 0.649$ s^{-1}, $\Delta A = -0.31$, $A_\infty = 0.13$, the residuals are shown at the bottom.

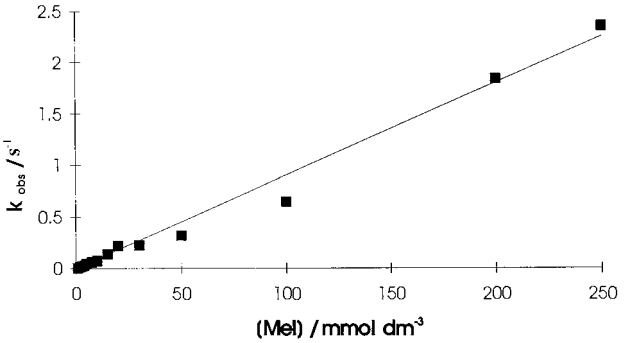

Fig. 2. Plot of k_{obs} versus [MeI] for reaction (1), in THF at 25°C. Concentration of complex (**1**) = 1.0×10^{-4} M.

The rate law for the second alkylation process is given by Eq. (4):

$$-\frac{d[Re]}{dt} = k_2[RX][Re(CN)(CNR)(dppe)_2] \quad (4)$$

The rate constant of the second alkylation reaction with RI (k_2) shows a marked influence of the nature of R (Figs. 2 and 3): $k_2 = 9.1 \pm 0.3$ (R = Me); 0.67 ± 0.03 (R = Et) and 0.45 ± 0.03 (R = Pr) dm^3 mol^{-1} s^{-1}, in a different order to that expected on the basis of the C-I dissociation energy (239.0, 233.3 or 233.1 kJ mol^{-1} for R = Me, Et or Pr, respectively [2]), but following the steric effects of R which appear to be the dominant ones. However, for EtBr, with a much higher C-halogen dissociation energy (292 kJ mol^{-1} [2]), the alkylation reaction is clearly slower ($3.32 \times 10^{-2} \pm 1.6 \times 10^{-4}$ dm^3 mol^{-1} s^{-1}).

Since the lowest concentration of MeI used was 1 mmol dm^{-3}, and even under these conditions the k_1 step is complete within the dead-time of the stopped-flow apparatus (2 ms) we can calculate that $k_1 \geq 3 \times 10^5$ dm^3 mol^{-1} s^{-1}.

In order to obtain further information on the alkylation kinetics we studied the effects of adding $[NBu_4]CN$, CNMe or NaI.

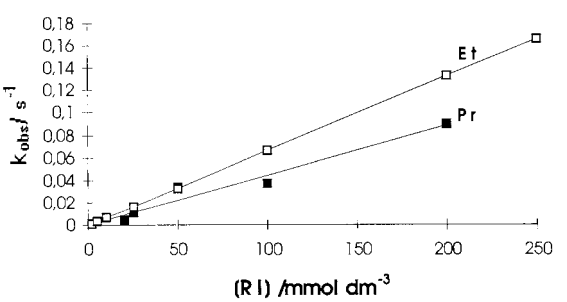

Fig. 3. Plot of k_{obs} versus [RI] (R = Et or Pr) for reaction (1), in THF at 25°C. Concentration of complex (**1**) = 1.0×10^{-4} M.

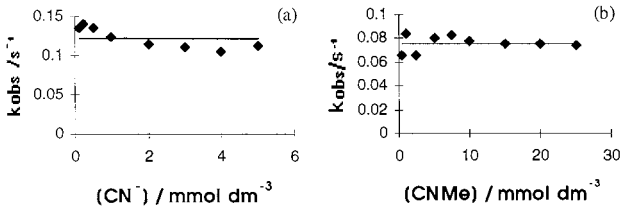

Fig. 4. Dependence of k_{obs} on (a) added cyanide or (b) methyl isocyanide for the reaction of (**1**) (1.0×10^{-4} M) with MeI (1.25×10^{-2} M and 1.0×10^{-2} M, respectively) in THF at 25°C.

At a constant concentration of $[NBu_4][trans\text{-}Re(CN)_2(dppe)_2]$ (**1**) and RX, the addition of CN^- or CNMe does not affect the rate of the reaction over the concentration range amenable to study as shown in Fig. 4(a) and (b).

However, added sodium iodide disturbs the alkylation process in a complicated way. We have shown that this complexity is attributable to the formation of Na^+ adducts as discussed below.

2.2. The reaction between trans-[Re(CN)$_2$(dppe)]$^-$ and MeI in the presence of NaI

The addition of an excess of NaI to the reaction between *trans*-$[Re(CN)_2(dppe)_2]^-$ (**1**) and MeI affects the rate as shown in Fig. 5.

Under these conditions, the absorbance–time curves are exponential, indicating a first order dependence on the concentration of complex. In addition the initial absorbance corresponds to that of (**1**).

Two features are evident from the data on Fig. 5: (i) at low concentrations of NaI, the value of k_{obs}/[MeI] is higher than that of k_2, and (ii) at high concentrations of NaI the MeI reaction is inhibited. Numerical analysis of these data results in the rate law shown in Eq. (5):

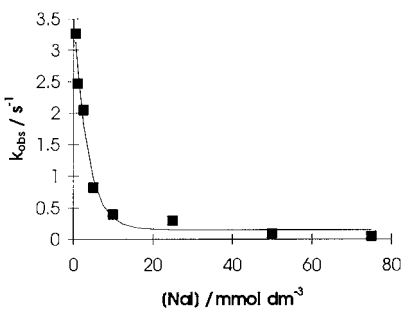

Fig. 5. Plot of k_{obs} versus [NaI] for the reaction of (**1**) (1.0×10^{-4} M) with MeI (2.5×10^{-2} M) in THF at 25°C.

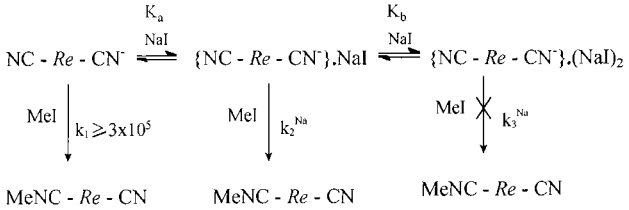

Scheme 1.

$$-\frac{d[Re(CN)_2(dppe)_2^-]}{dt} = \left\{\frac{(1.68 \pm 0.05) \times 10^3[MeI]}{1 + (4.8 \pm 0.9) \times 10^2[NaI]}\right\} \times [Re(CN)_2(dppe)_2^-] \quad (5)$$

This behaviour is consistent with the mechanism shown in Scheme 1, in which $Re = Re(dppe)_2$.

In this mechanism adduct formation between NaI and $[Re(CN)_2(dppe)_2]^-$ successively generates the species $[Re(CN)(CNNa)(dppe)_2]$ and $[Re(CNNa)_2(dppe)_2]^+$. In the first of these adducts it is to be expected that the electron-withdrawing Na^+ decreases the nucleophilicity of the CN ligands and that this effect is compounded for $[Re(CNNa)_2(dppe)_2]^+$.

The general rate law associated with the mechanism in Scheme 1 is presented in Eq. (6):

$$-\frac{d[Re(CN)_2(dppe)_2^-]}{dt} = \left\{\frac{k_1 + k_2^{Na}K_a[NaI] + k_3^{Na}K_aK_b[NaI]^2}{1 + K_a[NaI] + K_aK_b[NaI]^2}\right\} \times [MeI][Re(CN)_2(dppe)_2^-] \quad (6)$$

This rate law is derived assuming that formation of adducts are rapidly established equilibria. Inspection of the data in Fig. 5 shows that, even at the lowest concentration of NaI (0.5 mmol dm^{-3}) quantitative formation of $[Re(CN)(CNNa)(dppe)_2]$ occurs, indicating $K_a[NaI] > 1$ and $K_a \geq 2 \times 10^3$ dm^3 mol^{-1}. In addition, at high [NaI] the rate becomes vanishingly small with k_3^{Na} = insignificant. Thus, under the conditions our experiments were performed, Eq. (6) simplifies to Eq. (7):

$$-\frac{d[Re(CN)_2(dppe)_2^-]}{dt} = \frac{k_2^{Na}[MeI][Re(CN)_2(dppe)_2^-]}{1 + K_b[NaI]} \quad (7)$$

Comparison with Eq. (5) gives $k_2^{Na} = (1.68 \pm 0.05) \times 10^3$ dm^3 mol^{-1} s^{-1} and $K_b = (4.8 \pm 0.9) \times 10^2$ dm^3 mol^{-1}.

This interpretation of the effect of NaI on the reaction with MeI is intuitively reasonable with $k_1 \gg k_2^{Na} \gg k_3^{Na}$ and $K_a > K_b$.

The effect of ion-pairing on the nucleophilicity of metal complexes has been surveyed [3]. Further confirmation of our proposal comes from the isolation of a variety of adducts with mono-cations discussed below.

2.3. Reactions of the dicyano-complex with metal salts. Formation of the adducts trans-[Re(CN)(CNM)(dppe)$_2$] (M = Li, Na, Tl or Ag)

We have previously observed [1] that [NBu$_4$][*trans*-Re(CN)$_2$(dppe)$_2$] (**1**) reacts with Ag[BF$_4$] to give *trans*-[Re(CN)(CNAg)(dppe)$_2$], a rather insoluble and unstable species in solution. In the mass spectrum (FAB/MS) of this complex, the molecular ion (M^+ 1143, using a nitrobenzylic alcohol matrix) is clearly detected although displaying a much lower intensity than the fragment (1035) corresponding to the molecular ion of the much more stable compound [Re(CN)$_2$(dppe)$_2$] [4].

In order to get further evidence for the ability of **1** to react with metal salts with formation of adducts we investigated its reactions with MX (LiClO$_4$, NaI and TlBF$_4$). In general the reactions of MX with [Re(CN)$_2$(dppe)$_2$]$^-$ in THF afford products that are poorly soluble in the usual solvents and, upon attempted recrystallisation, undergo oxidation conceivably by adventitious oxygen to give *trans*-[Re(CN)$_2$-(dppe)$_2$], as observed [4] previously for the parent complex **1**, thus preventing their characterization by NMR spectroscopy. However, FAB/MS, elemental microanalysis and IR spectroscopy support their formulation as the adducts [Re(CN)(CNM)(dppe)$_2$] (**2**; M = Li, Na or Tl) formed according to reaction (8):

$$[NBu_4][\underset{(1)}{Re(CN)_2}(dppe)]_2 + MX \rightarrow [Re(CN)(\underset{(2)}{CNR})(dppe)_2] + [NBu_4]X \quad (8)$$

Hence, the molecular ions of the Li^+ and Na^+ adducts are clearly detected in their FAB/MS spectra at M^+ 1042 (1,4-butanediol as matrix) and 1058 (nitrobenzylic alcohol matrix), respectively, as well as the fragment $[M-M']^+$ (1035) corresponding to the molecular ion of the more stable decomposition product [Re(CN)$_2$(dppe)$_2$].

In the IR (KBr or Nujol) spectra of the adducts (**2**, M = Li, Na or Tl) a strong and broad band is observed at 1985, 1970 or 1945 cm^{-1}, respectively, being assigned to ν(CN). These values, as expected, are considerably lower than that of the dicyano Re(II) complex (2020 cm^{-1}) [4] but fall within the range observed for the Re(I) compounds **1** (1995 cm^{-1}) [4] and *trans*-[Re(CN)(CNMe)(dppe)$_2$] (2080, 1950 cm^{-1}).

2.4. Alkylation of [Re(CN)(CNNa)(dppe)$_2$]

[Re(CN)(CNNa)(dppe)$_2$] (**2**, M = Na) in THF, a solvent in which this complex dissolves slightly, is readily alkylated by MeI to afford *trans*-[Re(CNMe)$_2$(dppe)$_2$]$^+$ (reaction 9) which was previously obtained [5] upon replacement of chloride by CNMe at *trans*-[ReCl-(CNMe)(dppe)$_2$]:

$$\underset{(2,\ M=Na)}{trans\text{-}[Re(CN)(CNM)(dppe)_2]} + 2MeI \rightarrow trans\text{-}[Re(CNMe)_2(dppe)_2]I + NaI \quad (9)$$

The kinetics of this reaction were studied, by stopped-flow spectrophotometry, under similar experimental conditions to those used for the dicyano-complex (see above). The absorbance–time curves are a single exponential, indicating a first order dependence on the concentration of complex. However, the lower solubility of [Re(CN)(CNNa)(dppe)$_2$] in THF leads to very small absorbance changes ($\Delta A = 0.01$, compared with $\Delta A = 0.32$ for studies with [Re(CN)$_2$(dppe)$_2$]$^-$). This results in a large error for the rate constant. Over the concentration range, [MeI] + 0.25–2.5 mmol dm^{-3}, the kinetics follow a first order dependence on MeI ($k_4 = 70 \pm 20$ dm^3 mol^{-1} s^{-1}). This effect is qualitatively that predicted by our mechanism in Scheme 1 (i.e. $k_4 < k_1$). The difference between the values of k_2^{Na} and k_4 is presumably due to the use of NaI in the former and Na^+ in the latter.

The first alkylation of [Re(CN)(CNNa)(dppe)$_2$] is slower than the first alkylation of the anionic complex [Re(CN)$_2$(dppe)$_2$]$^-$, as expected, but faster than that of [Re(CN)(CNMe)(dppe)$_2$] (reaction 3) possibly on account of the significant ionic character of the CN–Na interaction which makes the CNNa ligand a better electron donor than CNMe. Moreover, the reaction of [Re(CN)(CNNa)(dppe)$_2$] with MeI produces [Re(C-NMe)$_2$(dppe)$_2$]$^+$ in a process associated with a single exponential, rate-limited by the first alkylation step. This indicates that the reaction of MeI with [Re(C-NMe)(CNNa)(dppe)$_2$]$^+$ is faster than MeI reacting with [Re(CN)(CNMe)(dppe)$_2$] (Eq. (3)). It seems likely that the Na^+ has a promoting effect on the H_3C–I bond cleavage process, possibly involving a transition state of the type shown below:

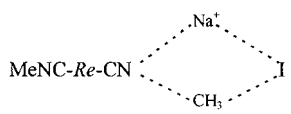

2.5. X-ray molecular structures of [NBu$_4$][trans-Re(CN)$_2$(dppe)$_2$] and trans-[Re(CN)$_2$(dppe)$_2$]

X-ray diffraction analysis performed on a crystal of [NBu$_4$][*trans*-Re(CN)$_2$(dppe)$_2$] (**1**) showed that two molecules exist per unit cell and the compound displays a pseudo octahedral geometry (Fig. 6a) and crystallizes in the triclinic space group $P\bar{1}$.

The two cyanide ligands are mutually *trans* in both complexes and display a linear arrangement ($\angle$C1–Re–C2 = 178.1(14)°) around rhenium.

Selected bond angles and distances are displayed in Table 1, and the fractional atomic coordinates are available as supplementary material.

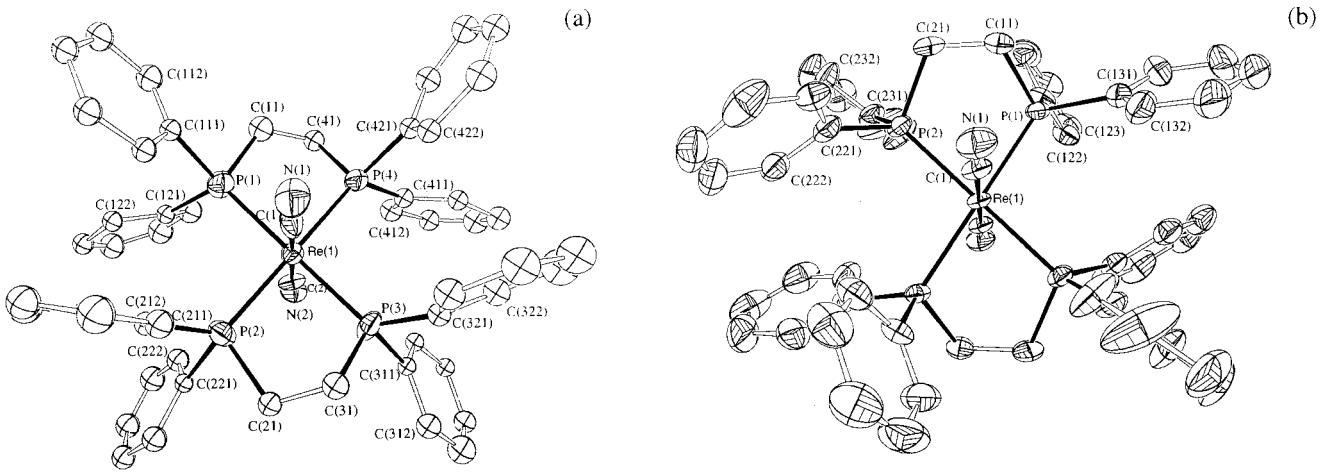

Fig. 6. ORTEP drawing of the anion [*trans*-$Re(CN)_2(dppe)_2]^-$ (a), and of *trans*-$[Re(CN)_2(dppe)_2]$ (b), showing the labeling schemes.

Table 1
Selected bond lengths (Å) and angles (°) for $[NBu_4]$-[*trans*-$Re(CN)_2(dppe)_2$] (**1**)

Re(1)–C(1)	2.10(3)
Re(1)–C(2)	2.08(3)
Re(2)–C(3)	2.09(3)
Re(2)–C(4)	2.10(3)
Re(1)–P(1)	2.381(8)
Re(1)–P(2)	2.379(8)
Re(1)–P(3)	2.347(8)
Re(1)–P(4)	2.366(8)
Re(2)–P(5)	2.370(8)
Re(2)–P(6)	2.377(8)
Re(2)–P(7)	2.356(8)
Re(2)–P(8)	2.373(8)
N(1)–C(1)	1.15(3)
N(2)–C(2)	1.16(3)
N(3)–C(3)	1.18(3)
N(4)–C(4)	1.16(3)
C(11)–C(41)	1.37(3)
C(21)–C(31)	1.46(3)
C(51)–C(61)	1.45(4)
C(71)–C(81)	1.48(3)
P–C (average)	1.84
C(2)–Re(1)–C(1)	178(1)
C(3)–Re(2)–C(4)	179(1)
Re(1)–C(1)–N(1)	178(3)
Re(1)–C(2)–N(2)	174(2)
Re(2)–C(3)–N(3)	177(3)
Re(2)–C(4)–N(4)	177(3)

The single crystal X-ray diffraction analysis of *trans*-$[Re(CN)_2(dppe)_2]$ showed it crystallizes in the monoclinic space group $P2_1/c$ and displays an octhedral geometry (Fig. 6b).

The two cyanide ligands also occupy the *trans* position to each other and the molecule presents a centre of inversion.

Selected bond angles and distances are displayed in Table 2, and the fractional atomic coordinates are available as supplementary material.

These two complexes crystallise in different space groups and display considerably different Re–P bond lengths which are shorter in the former, Re(I), complex (2.34–2.38 Å) than in the latter, Re(II), compound (2.41–2.42 Å). The values measured for the Re(II) complex are in excellent agreement with those previously reported for the related complex *trans*-$[ReCl_2(dppe)_2]$ (Re–P = 2.41–2.42 Å) [5]. A related decrease of ca. 0.1 Å on the M–P bond length upon addition of one electron to the metal site was previously recognized [6] for Re(III) or Mo(III) complexes with the $\{M(dppe)_2\}$ skeleton.

In contrast, no effect is observed on the Re–C bond lengths at the Re(I) or Re(II) cyanide complexes, 2.10(3) and 2.08(1) Å, respectively. Comparatively, the Re–C bond length (2.005(5) Å) measured on the related isocyanide complex *trans*-$[Re(CNEt)_2(dppe)_2]$-$[PF_6]$ is considerably shorter as a consequence of the better electron withdrawing properties of isocyanide compared to cyanide.

Table 2
Selected bond lengths (Å) and angles (°) for *trans*-$[Re(CN)_2(dppe)_2]$

Re(1)–C(1)	2.08(1)
Re(1)–P(1)	2.410(3)
Re(1)–P(2)	2.417(3)
C(11)–C(21)	1.54(2)
C(1)–N(1)	1.17(1)
P–C (average)	1.83
P(1)–Re(1)–P(2)	79.4(1)
Re(1)–C(1)–N(1)	176.0(10)

3. Experimental

All the solutions were prepared under dinitrogen. The solvent (THF) was dried by standard methods and distilled immediately before use. [NBu_4][*trans*-$Re(CN)_2(dppe)_2$] [4], *trans*-[$Re(CN)_2(dppe)_2$] [4] and *trans*-[Re(CN)(CNAg)$(dppe)_2$] [1] were prepared by published methods. The kinetics were performed on a Cantebury SF-40, from HI-TECH Scientifics at 25°C, monitoring the absorbance changes associated with the rhenium complexes at $\lambda = 400$ nm.

The absorbance–time traces were single exponential in all cases and the rate constants, together with the initial and the final absorbances, were computed by use of the Rapid Kinetics Software Suite (version 1.0) program on a City Desk 386-SX computer interfaced to the stopped-flow spectrophotometer. Curves were exponential for at least three half-lives. Typical absorbance–time curves for [NBu_4][*trans*-$Re(CN)_2(dppe)_2$] are shown in Fig. 1.

3.1. [Re(CN)(CNLi)$(dppe)_2$]

THF (20 cm^3) was added to a mixture [NBu_4][*trans*-$Re(CN)_2(dppe)_2$] (35 mg, 0.027 mmol) and $LiClO_4$ (6.0 mg, 0.065 mmol) and the mixture stirred overnight. The light orange solid was filtered off and dried under vacuum (20 mg, 71% yield).

FAB/MS (1,4-butanediol matrix): 1042 (M^+), 1035 ($M-Li^+$). Elemental analysis: Found (Calc.): %C, 62.4 (62.2); %N, 2.5 (2.7); %H, 4.8 (4.6).

3.2. [Re(CN)(CNNa)$(dppe)_2$]

THF (10 cm^3) was added to a mixture of [NBu_4][*trans*-$Re(CN)_2(dppe)_2$] (102 mg, 0.080 mmol) and NaI (13 mg, 0.087 mmol), and the mixture was stirred for 30 min at room temperature. The yellow suspension was filtered off and slightly washed with Et_2O (45 mg, 53% yield).

FAB/MS (nitrobenzylic alchool matrix): 1058 (M^+), 1035 ($M-Na^+$). Elemental analysis: Found (Calc. with 1/4NaI of crystallisation): %C, 58.8 (59.2); %N, 2.7 (2.6); %H, 4.6 (4.4).

3.3. [Re(CN)(CNTl)$(dppe)_2$]

THF (5 cm^3) was added to a mixture of [NBu_4][*trans*-$Re(CN)_2(dppe)_2$] (20 mg, 0.016 mmol) and $TlBF_4$ (15 mg, 0.051 mmol) and the suspension stirred for 1 h. The orange solid was filtered off and dried under vacuum (12 mg, 60% yield).

Elemental analysis: Found (Calc. with 1/10$TlBF_4$ of crystallisation): %C, 49.3 (49.2);%N, 1.9 (2.0);%H, 4.2 (3.8).

3.4. Structure solution and refinement for complexes

3.4.1. [NBu_4][*trans*-$Re(CN)_2(dppe)_2$]

The complex, $M_r = 2555$, crystallizes in the triclinic space $P\bar{1}$ with $a = 17.938(2)$, $b = 18.473(3)$, $c = 20.061(3)$ Å, $\alpha = 78.88(1)$, $\beta = 81.46(1)$, $\gamma = 85.76(1)°$, $V = 6443$ $Å^3$, $Z = 2$, $D_c = 1.32$ g cm^{-3}, $\mu(Mo-K_\alpha) = 20.3$ cm^{-1}.

Two molecules exist by unit cell, orientation matrix was obatined by least-squares refinement of 25 centred reflections with $14 < \theta < 17°$ and 17 877 independent reflections with $R_{int} = 0.036$ were collected in an Enraf-Nonius CAD4 diffractometer. 17 842 unique reflections with $F_2 \geq 0$ were used in structure solution and refinement of 725 parameters. The relative position of the Re atoms was found in a Patterson map and all the other non hydrogen atoms were located in subsquent difference Fourier maps. The Re, P and N atoms as well as the carbon in CN groups were refined isotropically. The hydrogen atoms of the anionic metal centre were inserted in calculated positions. The cation was refined without hydrogens. The weighting scheme $w = 1/[s^2(F_0^2) + (0.074*P)^2 + 80.4*P]$ $(P = F_0^2 + 2*F_c^2/3)$ was found to give an acceptable agreement analysis. Final refinement converged at $R_I = 0.05$ $(I > 2\sigma(I))$. The molecular structure is shown in Fig. 6(a) and final atomic coordinates for all the non hydrogen atoms are available as supplementary material.

3.4.2. *trans*-[$Re(CN)_2(dppe)_2$]

The complex, $M_r = 1035.02$, crystallises in the monoclinic space group $P2_1/c$ with $a = 11.673(2)$, $b = 13.302(3)$, $c = 17.166(4)$ Å, $\beta = 96.72(3)°$, $V = 2647(1)$ $Å^3$, $Z = 2$, $D_c = 1.30$ g cm^{-3}, $\mu(Mo-K_\alpha) = 24.5$ cm^{-1}. In a similar procedure to that of the previous compound, 9327 reflections $1.5 < \theta < 31.5°$ (4650 independent with $R_{int} = 0.07$) were collected by the ω-2θ scan mode, in an Enraf-Nonius TURBO CAD4 diffractometer equipped with a rotating anode (50 kV, 70 mA), using graphite monochromated radiation. Three standard reflections were monitored during data collection but no decay or instrumental instability was detected (the loss of intensity is less then 0.1%/h). Using the CAD4 software, data were corrected for Lorentz and polarization effects and empirically for absorption (minimum transmission factor 68%, average transmission factor 84%). 4200 unique reflections with $F^2 \geq 0$ were used in structure solution and refinement of 277 parameters. The position of the Re atom was obtained by a tridimensional Patterson synthesis and was found to be located at the special position $\bar{1}$. All the other non-hydrogen atoms were located in subsequent difference Fourier maps and refined with anisotropic thermal motion parameters. The hydrogen atoms were inserted in calculated positions and refined with fixed distances (1.08 Å) to the parent carbon atom. The weighting

scheme $w = 1/[s^2(F_o^2) + (0.1188*P)^2 + 13.7*P](P + F_o^2 + 2*F_c^2/3)$ was found to give an acceptable agreement analyses. Final refinement converged at $R_1 = 0.07$ ($I > 2\sigma(I)$). The molecular structure is shown in Fig. 6(b) and final atomic coordinates for all the non hydrogen atoms are given in Table 2.

Lists of observed and calculated structure factors, for both structures, tables of anisotropic thermal parameters, hydrogen atomic coordinates, bond lengths are avaiable as suplementary material. The structure solution and refinement were done with SHELX93 [7] and the illustrations were drawn with ORTEP-II [8]. The atomic scattering factors and anomalous scattering terms were taken from International Tables [9].

4. Supplementary material

Ten tables with kinetic data are available as well as tables with the fractional atomic coordinates for each of the two X-ray structures.

Acknowledgements

This work was partially supported by the Junta Nacional de Investigação Científica e Tecnológica (JNICT), the Fundação para a Ciência e Tecnologia (FCT), the PRAXIS XXI programme (Portugal) and the Instituto de Cooperação Científica e Tecnológica Internacional (ICCTI)/The British Council protocol.

References

[1] M.F.N.N. Carvalho, M.T. Duarte, A.M. Galvão, A.J.L. Pombeiro, J. Organometal. Chem. 511 (1996) 163.
[2] D.R. Lide (Ed.), Handbook of Chemistry and Physics, 74th Edn., CRC Press, Boca Raton, 1993–4.
[3] S. Henderson, R.A. Henderson, Adv. Phys. Org. Chem. 23 (1987) 1, and references therein.
[4] M.F.N.N. Carvalho, M.T. Duarte, A.M. Galvão, A.J.L. Pombeiro, J. Organometal. Chem. 469 (1994) 79.
[5] M.F.N.N. Carvalho, A.J.L. Pombeiro, J. Chem. Soc. Dalton Trans. (1989) 1209.
[6] T.Al Salih, M.T.Duarte, J.J.R. Fraústo da Silva, A. M. Galvão, M.F.C. Guedes da Silva, P.B. Hitchcock, D.L. Hughes, C.J. Pickett, A.J.L. Pombeiro, R.L. Richards, J. Chem. Soc. Dalton Trans. (1993) 3015.
[7] G.M. Scheldrick, SHELX93; Crystallographic Calculation Program, University of Cambridge, 1993.
[8] C.K. Johnson, ORTEP-II, Report ORNL-5138, Oak Ridge National Laboratory, Park Ridge, TN, 1976.
[9] T. Hahn (Ed.), International Tables for Crystallography, vol. A, Reidel, Dordrecht, 1983.